ORIGINAL ARTICLE

Jan Idkowiak · Gunnar Weisheit · Juliane Plitzner ·
Christoph Viebahn

Hypoblast controls mesoderm generation and axial patterning in the gastrulating rabbit embryo

Abstract Gastrulation in higher vertebrate species classically commences with the generation of mesoderm cells in the primitive streak by epithelio-mesenchymal transformation of epiblast cells. However, the primitive streak also marks, with its longitudinal orientation in the posterior part of the conceptus, the anterior-posterior (or head-tail) axis of the embryo. Results obtained in chick and mouse suggest that signals secreted by the hypoblast (or visceral endoderm), the extraembryonic tissue covering the epiblast ventrally, antagonise the mesoderm induction cascade in the anterior part of the epiblast and thereby restrict streak development to the posterior pole (and possibly initiate head development anteriorly). In this paper we took advantage of the disc-shape morphology of the rabbit gastrula for defining the expression compartments of the signalling molecules Cerberus and Dickkopf at pregastrulation and early gastrulation stages in a mammal other than the mouse. The two molecules are expressed in novel expression compartments in a complementary fashion both in the hypoblast and in the emerging primitive streak. In loss-of-function experiments, carried out in a New-type culturing system, hypoblast was removed prior to culture at defined stages before and at the beginning of gastrulation. The epiblast shows a stage-dependent and topographically restricted susceptibility to express *Brachyury*, a T-box gene pivotal for mesoderm formation, and to transform into (histologically proven) mesoderm. These results confirm for the mammalian embryo that the anterior-posterior axis of the conceptus is formed first as a molecular prepattern in the hypoblast and then irrevocably fixed, under the control of signals secreted from the hypoblast, by epithelio-mesenchymal transformation (primitive streak formation) in the epiblast.

Keywords Epiblast · Cerberus · Dickkopf · Polarity · Rabbit

Edited by D. Tautz

J. Idkowiak
Department of Anatomy and Cell Biology, Martin-Luther-University,
Grosse Steinstrasse 52,
06097 Halle, Germany

G. Weisheit
Department of Anatomy, Anatomy and Cell Biology,
University of Bonn,
Nussallee 10,
53115 Bonn, Germany

J. Plitzner · C. Viebahn (✉)
Department of Anatomy and Embryology, Georg-August-University,
Kreuzbergring 36,
37075 Göttingen, Germany
e-mail: cviebah@gwdg.de
Tel.: +1-49-551-397001
Fax: +1-49-551-397043

Introduction

A common characteristic in early development of most animal species consists of a principal conversion of the early conceptus during the gastrulation process. This conversion seems to follow three major aims: (1) the internal milieu of the embryo is established by differentiation of the three germ-layers ectoderm, mesoderm and endoderm; (2) the main body axes, namely the anterior-posterior (head-tail) and, consequently, the left-right axis, are definitely fixed in the geometrical sense; and (3) the arrangement of the organ anlagen, the future body plan, is laid down. As part of the first aim many cells undergo—for the first time in development—a fundamental change in shape and transform from a polarised into an unpolarised conformation. In fact, gastrulation commences with the generation of unpolarised mesoderm cells in a two-layered embryo; originating from the polarised epiblast epithelium (the upper layer) by epithelio-mesenchymal transformation mesoderm cells disseminate between the epiblast and the hypoblast (the lower layer), a mechanism that is well conserved throughout the animal kingdom (Hay 1995; Viebahn 1995; Wodarz et al. 1995). In amniotes, mesoderm cells are generated first in the posterior part of the conceptus in a longitudinal band of

increased cell density called the primitive streak (Bellairs 1986; Viebahn 1995). The (molecular) patterning mechanisms restricting the development of the primitive streak to the posterior part of the embryo and establishing a definitive posterior (tail) and anterior (head) identity are amongst the most complex and fascinating matters occupying investigators in developmental biology to date and are the subject of the present report.

Molecular mechanisms of gastrulation processes in mammals have been well investigated in the mouse (Beddington and Robertson 1998; Tam and Gad 2004). A wealth of molecular data and knock-out phenotypes suggest an important role of the visceral endoderm, an extraembryonic tissue covering the embryonic area and the equivalent of the hypoblast in other mammals, in orchestration of mesoderm generation and head formation. Firstly, "organizer genes" are expressed in the anterior part of the mouse hypoblast (anterior visceral endoderm, AVE) before primitive streak formation. Amongst these genes are the homedomain containing transcription factor *goosecoid* (Blum et al. 1992; Filosa et al. 1997), the LIM-homeodomain containing transcription factor *Lim1* (Barnes et al. 1994; Shawlot and Behringer 1995) and the winged helix protein *Hnf3β* (Ang et al. 1993; Monaghan et al. 1993; Sasaki and Hogan 1993; Filosa et al. 1997). These genes are expressed in the frog organizer, which induces secondary axis if grafted ectopically (reviewed in Weinstein and Hemmati-Brivanlou 1999; de Robertis et al. 2000). The mouse equivalents of these genes are expressed in the AVE, but also in Hensen's node and in the anterior primitive streak suggesting that more than one organizer structure—as is the case in amphibians—are expected to be operating in mammals (reviewed in Beddington and Robertson 1999). Secondly, the AVE expresses secreted molecules that might act on the adjacent epiblast such as the Wnt-antagonist *Dickkopf1* (*Dkk1*: Glinka et al. 1998), the BMP and nodal antagonist *Cerberus-related1* (*Cer1*: Belo et al. 1997; Biben et al. 1998; Pearce et al. 1999) and the TGFβ superfamily genes *nodal* and *Lefty1* (Conlon et al. 1994; Meno et al. 1996; Varlet et al. 1997; Oulad-Abdelghani et al. 1998). *Dickkopf* and *Cerberus*, both originally discovered in the frog, are causally involved in head induction (Bouwmeester et al. 1996; Glinka et al. 1998). As both antagonise pathways involved in the mesoderm programme, namely nodal and Wnt signalling, one model, which is also supported by strong evidence obtained in the chick (Foley et al. 2000; Bertocchini and Stern 2002), suggests that they suppress mesoderm generation anteriorly (with the result of primitive streak formation posteriorly) and consequently "allow" execution of the head-development programme (Kimura et al. 2000; Perea-Gomez et al. 2001a, 2002).

Experiments on the inductive capabilities of the hypoblast/visceral endoderm were carried out both in the mouse and the rabbit. The forebrain marker *Hesx1* could not be detected in the neurulating mouse embryo after surgical removal of the hypoblast in early gastrulation stages (Thomas and Beddington 1996). Moreover, the mesoderm marker *Brachyury* was ectopically expressed in mouse egg cylinders after removal of visceral endoderm (Perea-Gomez et al. 2001b) and AVE explants are able to suppress *Brachyury* and *cripto* expression in epiblast tissues (Kimura et al. 2000). In the context of head development, hypoblast explants of rabbit pre-gastrulation stages can induce ectopic anterior neural development if grafted in the extraembryonic ectoderm of chick embryos (Knoetgen et al. 2000). However, these studies leave many questions unanswered as to how primitive streak formation, and hence the gastrulation process, is initially restricted to the posterior pole of the embryonic area, namely whether a topographic distribution exists within the hypoblast with regard to the inductive capabilities mentioned above.

To start finding answers to these two questions we took advantage of the disc-shaped morphology of the rabbit embryonic area and the fact that in this species several developmental stages can be recognized in vivo prior to primitive streak (and hence mesoderm) formation (Viebahn et al. 2002). Characterising the expression patterns of the rabbit orthologues of the inhibitory molecules *Dkk1* and *Cer1* before and at the beginning of streak formation, we could identify novel expression compartments in the anterior hypoblast and in the primitive streak. Apart from this, hypoblast was totally removed before and at the beginning of mesoderm formation and the epiblast with remaining extraembryonic tissues still attached was cultured overnight in a novel New-type culture adapted for the rabbit embryo. The effect of the experimental procedure on the mesoderm programme was assessed at the molecular level using the mesoderm marker *Brachyury* in whole-mount in situ hybridisation and at the histological level using resin embedding of the hybridised embryos. From stage-dependent changes in mesoderm formation after hypoblast removal we conclude that the patterning mechanisms for mesoderm formation are laid down earlier and in a topographically more restricted fashion in the mammalian embryo than hitherto believed and that gastrulation is initiated and commences prior to primitive streak formation.

Materials and methods

Animals

The uteri of naturally mated pregnant New Zealand White rabbits (Lammers, Euskirchen) were dissected after applying an overdose (90 mg) of Narcoren (Bayer Veterinärmedizin, Munich, Germany) intravenously. Blastocysts (8–15 per litter) were flushed from the uterus at 6.0 to 6.5 day post conception (dpc) using warm (37°C) phosphate-buffered saline (PBS). After washing the embryos twice to remove blood and cellular debris blastocysts were transferred into petri dishes containing full medium [HAM's F10 supplemented with 20% fetal calf serum (FCS); Biochrom, Berlin, Germany] and kept in an incubator (37°C, 5% CO_2) prior to dissection.

Manipulation and culture conditions

The developmental age of the embryo (stage 1 to 3) was assessed under dark field optics according to the presence or absence of the anterior marginal crescent (AMC) and the posterior gastrula extension (PGE) as described previously (Viebahn et al. 2002). Next, the anterior pole of the embryonic disc was marked by piercing the extraembryonic tissue just outside the AMC to be able to determine the anterior-posterior axis during the ensuing embryo culture. Subsequently, a blastocyst fragment containing the embryonic disc surrounded by a broad band of extraembryonic tissue was dissected from blastocysts in full medium at room temperature using iridectomy scissors and flame-polished tungsten needles.

Following a protocol for culturing chick embryos (New 1955), embryonic discs were submerged in about 500 μl full medium in an organ culture dish (5 cm in diameter, Falcon, Heidelberg, Germany; Fig. 1a), and placed with the hypoblast side up on a 20 μl drop of agarose (0.5% in PBS; BioRad, Wien, Austria) which had been placed on another agarose drop (measuring 70 μl) previously. The amount of medium was then carefully reduced using a drawn-out Pasteur pipette to the point that the explanted tissue was exposed to air and did not come in touch directly with the surface of the culturing medium. In this way, the tissue was kept flat during the culture period and was prevented from floating off the agarose drop.

Before further manipulation, the anterior pole of the disc was permanently stained in the adjacent extraembryonic tissue using a few crystals of water-insoluble carmine (Sigma, C-1022). Using flame-polished tungsten needles and dark-field illumination in a dissecting microscope the
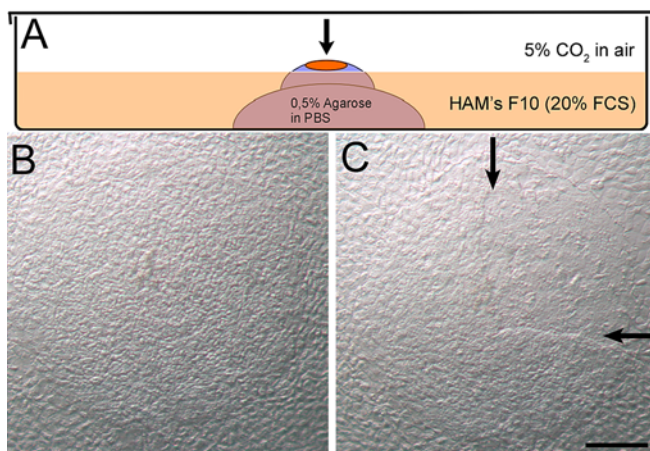

Fig. 1 Schematic illustration (cross section) of the experimental setting: explants mounted ventral (hypoblast) surface up on agarose drops in culture dishes filled with medium, the fluid level almost touching the cut edge of the tissue (**a**). En face views (**b**, **c**; angle of vision indicated by the *arrow* in **a**) of a stage-2 rabbit embryo in bright-field illumination of the dissecting microscope before (**b**) and after (**c**) partial resection of the hypoblast illustrating the different appearance of ventral hypoblast (to the *left* and *below arrows* in **c**) and epiblast (to the *right* and *above arrows* in **c**) surface. Peripheral to the round embryonic disc the ventral layer (yolk sac epithelium) is still intact. *Scale bar* 125 μm

hypoblast was circumferentially cut at the border of the embryonic disc and lifted off either as a whole or in several segments. Presence and absence of the hypoblast could be observed due to the different optical appearance of the embryonic disc before (Fig. 2a) and after (e.g. right anterior quadrant in Fig. 2b) removal of the hypoblast. In this way, it was confirmed that the lower layer (hypoblast and a small rim of adjoining yolk sac epithelium) was removed from the whole embryonic disc area. As controls, embryonic discs were mounted on agarose without manipulating the hypoblast at all. To exclude the possibility that mere mechanical disturbance of the embryo may cause the experimental results described below, the following more stringent sham operations were carried out in 16 stage-1 embryonic discs: the hypoblast was incised circumferentially and then either left in place (3/16) or replaced after having been lifted off almost completely (13/16). Cultures were incubated at 37°C/5% CO_2 and 100% humidity for approximately 16 h. After incubation embryos were fixed in 4% paraformaldedhyde (PFA) in PBS for 1 h, dehydrated and stored in methanol (−20°C) until use for in situ hybridisation. See Fig. 7 for number of manipulated and analysed embryonic discs.

PCR cloning of rabbit gene probes

Human, mouse and chicken cDNA sequences were aligned to select typically three pairs of "nested" degenerated primers per gene, which were used in different combinations. PCR products of the correct size were cloned and sequenced on both strands following standard PCR conditions (35 cycles at 95°C for 30 s, 60°C for 1 min and 72°C for 2 min). Successful primer combinations were as follows: *Cer1* (687 bp): 5′-TTG TTC TCT TGC CTY TRG GRA ARR C (forward), 5′-CAC TGT CAC TCY ACY WGC ATN ACC (reverse). *Dkk1* (481 bp): 5′-ATT CCA ACG CTA TCA ARA AYY TNC C (forward), TTA GTA CAG GTT TAC AGA TYT TNS WCC A (reverse). *Brachyury* (635 bp): 5′-CTC ACC AAC AAG CTC AAT GGA-3′ (forward), 5′-GAT GGT ACC ATT GCT CAC AGA CC (reverse).

In situ hybridisation and histology

All chemicals were purchased from Sigma (Munich, Germany) if not stated otherwise. Standard in situ hybridisation protocols (Lowe et al. 1996; Belo et al. 1997) were adapted for the requirements of rabbit embryos (Weisheit et al. 2002). Protease treatment (10 μg/ml proteinase K in PBS; Roche, Mannheim) depended on the developmental age: 1–2 min for stage 1 embryos and 3–5 min for stage 2 to 4 and cultured embryos. Hybridisation buffer contained 50% formamide, 1.3× SSC pH 4.5, 5 mM EDTA, 50 μg/ml tRNA, 0.2% Tween 20, 0.5% CHAPS and 50 μl/ml heparin. Embryos were placed in nylon baskets and transferred to sterile screw-top PVC tubes (Bibby-Sterilin, Staffordshire, UK) during the pre-hybrid-
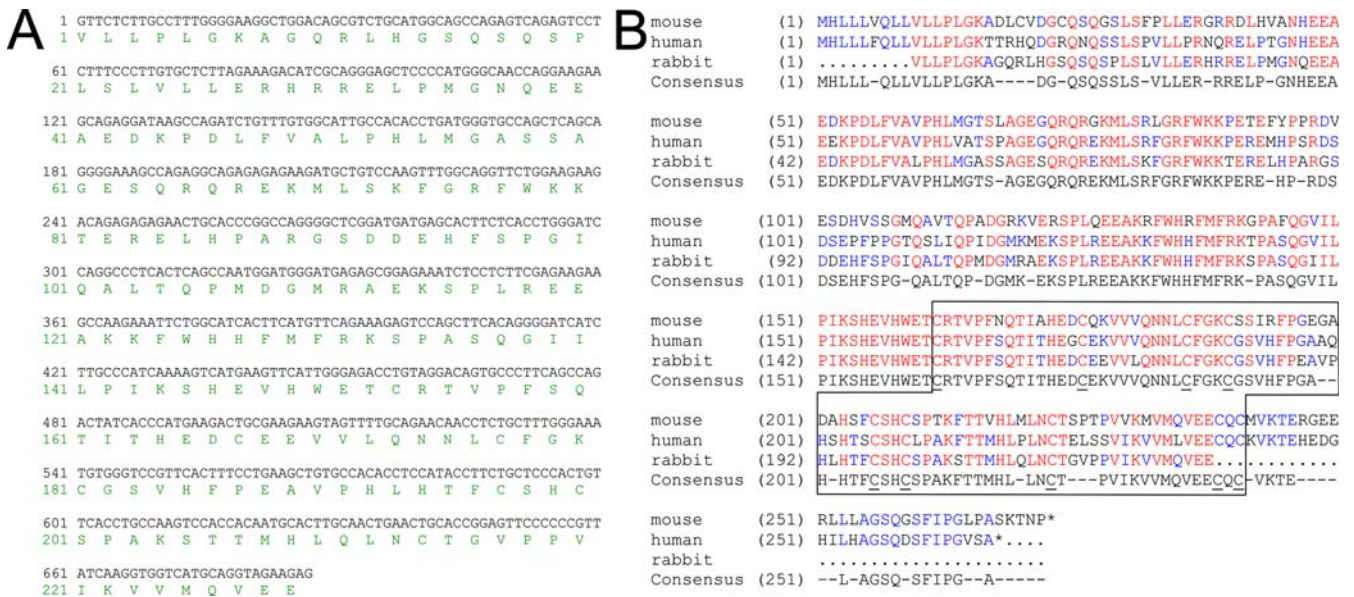
Fig. 2 Rabbit *Cer1* (*rbCer1*) cDNA and predicted protein sequence (**a**); interspecific comparison (**b**). Amino acids conserved in all three species shown are highlighted in *red*, those conserved in only two of the species shown are highlighted in *blue*. The *black box* in **b** marks the cysteine-rich domain with the conserved cysteine residues *underlined* in the consensus sequence [*asterisks* mark stop-codons; *mouse*: *Mus musculus musculus* (accession number NM_034017), *human*: *Homo sapiens* (accession number NP_005445), *rabbit*: *Oryctolagus cuniculus* (accession number AY 570542)]

isation (70°C for 1 h) and hybridisation (70°C overnight) procedure. The hybridisation buffer contained 0.4 µg/ml digoxigenin-labelled RNA (denatured for 2 min at 95°C). Following washing procedures in hybridisation buffer and MABT (100 mM maleic acid, 150 mM NaCl, 0.1% Tween, pH 7.5) hybridised RNA was visualised using anti-digoxigenin antibody coupled to alkaline phosphatase and BM-purple substrate (both Roche, Mannheim, Germany). The reaction was initiated by transferring embryos to petri dishes filled with the substrate and was allowed to proceed for 6–48 h at room temperature. Embryos were photographed in Mowiol under a cover glass. For histological analysis and localisation of staining reactions embryos were dehydrated in methanol and embedded in Technovit 8000 (Heraeus-Kulzer, Werheim, Germany) at 4°C in empty tablet moulds. Transverse or sagittal sections of the embryonic discs were made at 5 µm using glass knifes.

Results

Dkk1 and *Cer1* are expressed in anterior parts of the hypoblast

The rabbit *Cerberus-related1* (*rbCer1*) cDNA clone obtained by RT-PCR (accession no. AY 570542) comprises 687 bp of the open reading frame (Fig.2a). The predicted rbCer1 amino acid sequence begins at position 10 and ends at position 238, which is three amino acids upstream of the end of the cysteine-rich domain (black box in Fig. 2b) of the consensus Cer1 protein. An alignment of the predicted rabbit Cer1 protein shows high homology to the known mammalian orthologues (Fig.2b; percent sequence similarities: *Homo sapiens* 82.5%, accession

no. NP_005445; *Mus musculus* 77.7%, accession no. NM_034017). The cysteine-rich domain is highly conserved in all Cer1 orthologues and frog Cerberus; within the cysteine-rich domain the sequences share a conserved spacing of nine cysteine residues. Seven of these cysteines are included in our *rbCer1* clone and this domain shows 62% sequence similarity to Cerberus protein of the frog (*Xenopus laevis*, accession no. BAC 54274). The structure of *rbDkk1* cDNA and protein (accession no. AY575211) will be published elsewhere (Weisheit et al., in preparation). To visualise the expression patterns, digoxigenin-marked RNA probes of *rbDkk1* (534 bp) and *rbCer1* (687 bp) generated from these cDNAs were used.

Both genes are expressed at all stages analysed in this study and show expression domains at first in the hypoblast and later also in the primitive streak (Fig. 3). At stage 1, which is defined by the appearance of the anterior marginal crescent (AMC), *rbCer1*-expressing hypoblast cells form a mushroom-like pattern with a clear anteroposterior polarisation (Fig. 3a). Anteriorly, the domain is limited by a narrow band of hypoblast cells not expressing *rbCer1* (Fig. 3d); posteriorly, the mushroom-shape is created by two "shoulders" of non-expressing hypoblast cells (Fig. 3a) and a "stem" of *rbCer1*-expressing hypoblast cells reaching well into the centre of the embryonic disc. At stage 2, which is characterised by a crescent of lower cell density at the posterior pole of the disc called the posterior gastrula extension (PGE), the *rbCer1* domain does not change its general shape (Fig. 3b). Its anterior circumference is still separated from the border with the extra-embryonic tissue by several rows of hypoblast cells not expressing *rbCer1*. With the appearance of the primitive streak at stage 3 the mushroom-like domain decreases in size, rounds up—

frequently dominating the left anterior quadrant of the embryonic disc—and the *rbCer1* expression level is reduced. Simultaneously, a new domain is formed in the anterior part of the primitive streak (Fig. 3c, e, f): strong expression of *rbCer1* is found in apical parts of epiblast cells undergoing epithelio-mesenchymal transformation while a weaker expression is found in the basal compartment of these cells (Fig. 3f); the hypoblast does not express *rbCer1* in this posterior domain (arrowheads in Fig. 3f). When the primitive streak is elongated to its full extent at late stage 3 and stage 4 (primitive node stage), the *rbCerl*-expressing domain is found to cover the entire streak (not shown).

The *rbDkk1* domain at stage 1 has a clasp-like shape with a crescent which is narrowest at the anterior pole (Fig. 3g). From the lateral parts of this crescent two

Fig. 3 Expression of *rbCer1* (**a–f**) and *rbDkk1* (**g–l**) in rabbit embryonic discs: *en face* views (**a–c** and **g–i**) and 5-μm sections (**d–f** and **j–l**) from stage 1 to stage 3 (at 6.0–6.5 dpc) as analysed by in situ hybridisation. The outlines of the embryonic discs are indicated by *dotted lines* in **a–c** and **g–i**. All sections are orientated with the anterior pole to the *left* and the epiblast (*e*) to the *top*. *Arabic numerals* indicate the stage; *bars* and *letters* indicate the positions of sagittal sections shown; *boxes* in **e** and **k** indicate the position of magnified details in **f** and **l**; *asterisks* mark the border of the embryonic disc, *arrowheads* mark hypoblast cells; *h* hypoblast side, + mesoderm cells. *Scale bar* 170 μm in **a–c** and **g–i**; 50 μm in **d**, **e**, **j**, **k**; 10 μm in **f**, **l**
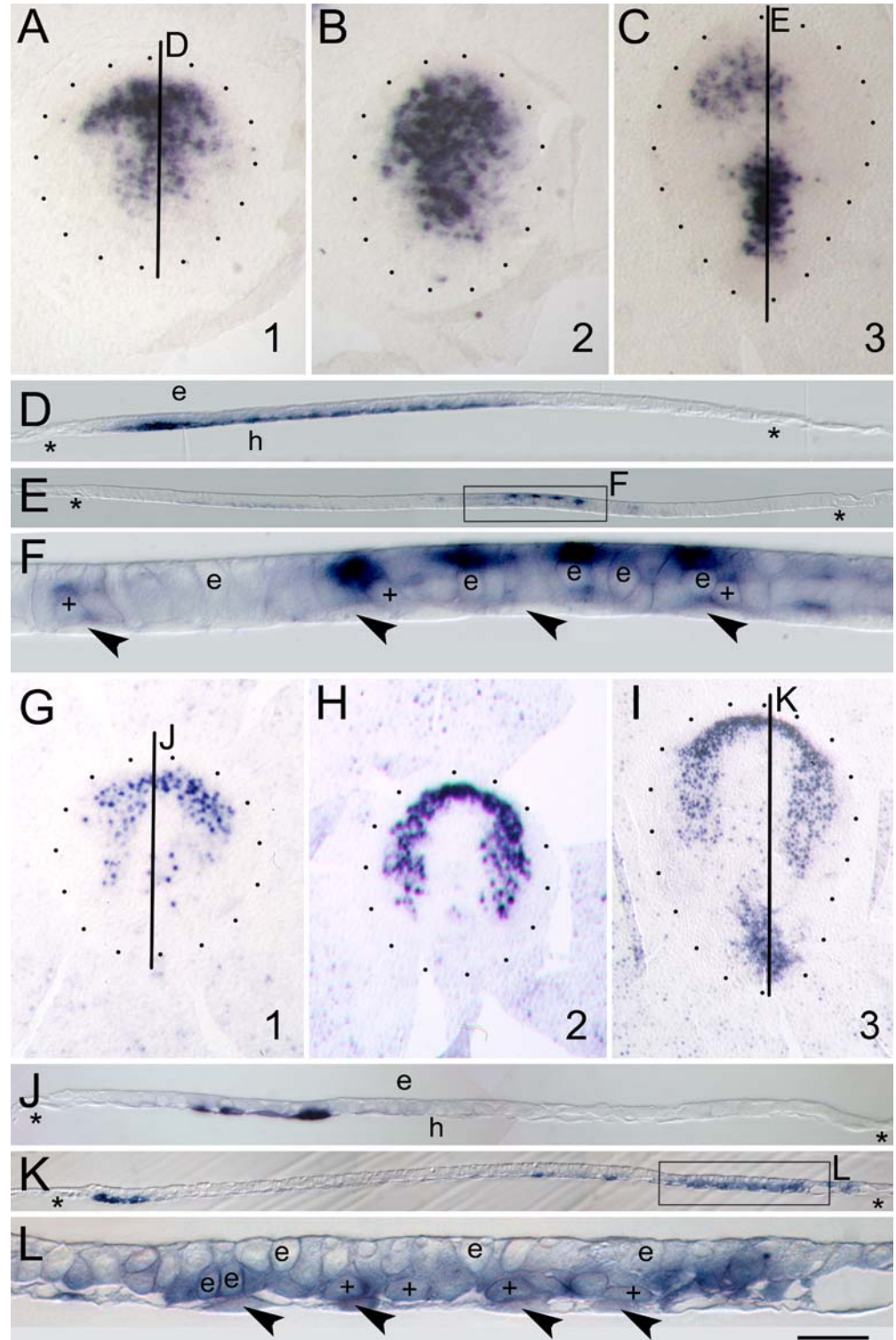
branches fan out towards the posterolateral halves of the embryonic disc. The *Dkk1* expression domain is confined to the hypoblast (Fig. 3j) and separated by several rows of hypoblast cells from the embryonic-extraembryonic border of the disc (Fig. 3j, k) as is the case with the *rbCer1* domain (Fig. 3a, b). This pattern retains its principal shape at stage 2 and 3, where the most anterior crescent-like sector only consists of four to five rows of hypoblast cells (Fig. 3j, k) and the lateral trail-like extensions are wider and less dense than at stage 1 (Fig. 3h, i). At all stages the clasp-shape surrounds a central and anterior region of the hypoblast that is free of *rbDkk1*-expressing cells (Fig. 3g–i). Similar to the *rbCer1* expression pattern an additional *rbDkk1* domain is seen when the primitive streak appears. However, the *rbDkk1* domain lies in the posterior half of the primitive streak only to some extent overlapping the *rbCer1*-expressing region. Within the primitive streak and beginning at the posterior pole of the embryonic disc at early stage 3, hypoblast, mesoderm and epiblast cells all express *rbDkk1*, but in a graded fashion (Fig. 3l): strong
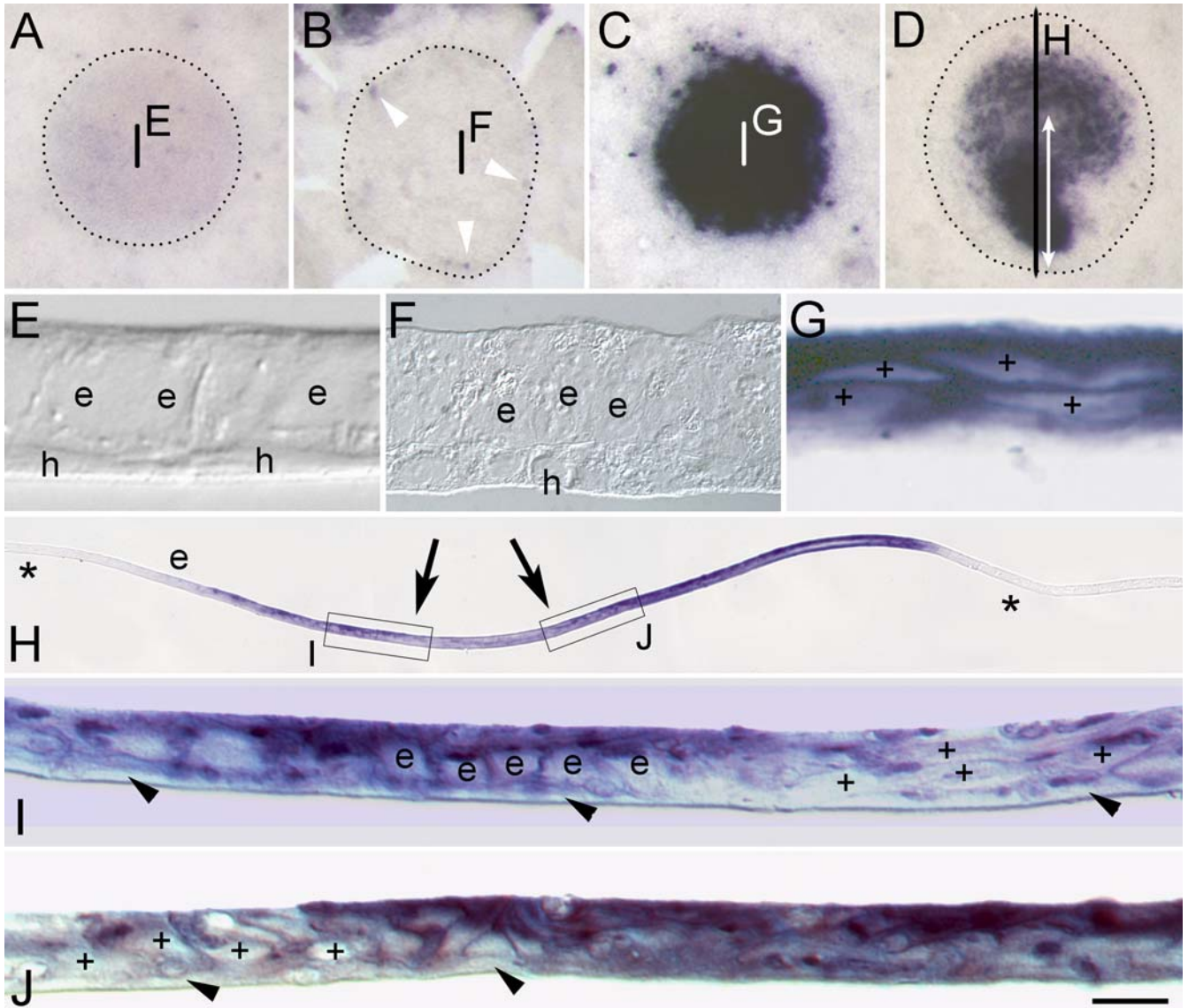

Fig. 4 *Brachyury* expression in embryos explanted at stage 1 and cultured with hypoblast in situ (controls: **a, e**), after sham operations of the hypoblast (**b, f**), or after total ablation of the hypoblast (**c, d, g–j**). *Bars* and *letters* in en face views (**a–d**) indicate position of sections shown in **e–j**; other inscriptions and orientation of sections as in Fig. 3. *Brachyury*-negative columnar epiblast cells (*e*) in the bilaminar disc of the control embryos (**a, b, e, f**) contrast with multilayered spindle-like mesoderm cells (+) strongly expressing *Brachyury* following hypoblast (*h*) ablation (**d, g, i, j**). *Arrowheads* (in **b**) indicate peripheral epiblast cells weakly expressing *Brachyury* following sham operations. A midsagittal section covering both the orthotopic and the ectopic *Brachyury* expression domains of embryos following hypoblast resection (**h–j**) shows the mesoderm cell layer to be continuous from the posterior pole to the anterior third of the disc (*left arrow* in **h**) and indicating the extent of an enlarged primitive streak (*white double arrow* in **d**). Mesoderm cells (+) in the anterior part of the streak (*between arrows* in **h**) express *Brachyury* less strongly than mesoderm cells in the posterior part (to the *right* in **j**) or than epiblast cells (*e*) in the ectopic expression domain (to the *left* in **i**). *Scale bar* 150 μm in **a–d**; 50 μm in **h**; 20 μm in **i, j**; 10 μm in **e-g**

expression is found in mesoderm, hypoblast and in the basal compartment of epiblast cells. Apically, the expression intensity decreases in the epiblast. In late streak stages the *rbDkk1* domain extends to more anterior parts of the streak until *rbDkk1* is expressed in the entire full-length streak area at stage 4 (Weisheit et al., in preparation).

Comparing the expression domains of *rbDkk1* and *rbCer1* it is noteworthy that both in the hypoblast and in the streak compartment the patterns are complementary to one another with a small but definite region of overlap: in the hypoblast layer, the posterior border of the *rbDkk1* expression domain touches and overlaps the sector in the anterior centre of the disc expressing *rbCer1* in the mushroom-like pattern. Similarly at stage 3, *rbCer1* is expressed in the anterior part and *rbDkk1* in the posterior part of the emerging primitive streak with the overlap extending further during streak elongation; while both epiblast and mesoderm cells express *rbCer1* and *rbDkk1* in this domain, the hypoblast layer expresses *rbDkk1* but not *rbCer1*. At the subcellular level, there seems to be a remarkable complementarity within the epiblast layer: *rbCer1* is expressed apically (Fig. 3f) while *Dkk1* is confined to basal compartments of epiblast cells (Fig. 3l).

Ectopic *Brachyury* expression following hypoblast removal

After removal of the hypoblast we found both ectopic and widened orthotopic expression patterns of the *Brachyury* gene in most embryonic discs but size and shape of the expression patterns depended on the stage of the embryo at the beginning of culture (Figs. 4, 5, 6).

In 24 of the 27 embryos in which the hypoblast was ablated at stage 1 *Brachyury* was expressed after 16 h of incubation (Fig. 7). As *Brachyury* expression starts physiologically within the PGE and later on is expressed in cells of the streak and the surrounding mesoderm we called any expression domain confined to the posterior quadrant an orthotopic domain (dark blue in Fig. 7). If *Brachyury* was expressed outside this orthotopic location, for example in central parts of the disc, which cannot be found in non-cultured embryos, we called this domain ectopic (light blue in Fig. 7). By these criteria, 14 embryos had an orthotopic domain strongly expressing *Brachyury* and 10 embryos had *Brachyury* transcripts in an ectopic domain but an orthotopic domain was missing; in 4 of these latter 10 embryos, *Brachyury* was expressed in the entire embryonic disc (Fig. 4c) whereas the other 6 showed a disc-like expression pattern in central parts that does not reach the embryonic border (not shown). Sections showed that in both these groups of embryos (orthotopic or ectopic expression patterns only) the areas of *Brachyury* expression regularly contained spindle-shaped flat cells resembling mesoderm cells (Fig. 4g). Ten embryos expressed *Brachyury* in both the orthotopic and in an ectopic domain (Fig. 4d, h–j). The expression was generally more intensive in the orthotopic than in the ectopic domain (Fig. 4d) showing multi-layered *Brachy-*

ury-expressing mesoderm cells and a strong apical staining in epiblast cells about to undergo epithelio-mesenchymal transition, respectively (Fig. 4j). The overwhelming cell type in the ectopic domain, which was less intensively stained, were large cuboidal, apically stained epiblast cells (Fig. 4i). Between these two domains, multi-layered mesoderm cells with a weak *Brachyury* expression were also regularly found (Fig. 4h, between the arrows, i, j). The area of expansion in these embryos, where histologically confirmed mesoderm cells had been generated, reaches from the most posterior end of the disc to anterior regions extending beyond the transverse diameter of the embryonic disc (white double arrow in Fig. 4d).

Histology of cultured embryos in which the hypoblast had been removed prior to culture confirmed the absence of hypoblast in areas with strong *Brachyury* expression and ongoing mesoderm formation in most cases (Fig. 4g, j). However a thin layer of squamous cells resembling hypoblast cells was frequently found in areas which showed ectopic *Brachyury* expression but no apparent mesoderm formation (Fig. 4i, j).

Control stage-1 embryos with an intact hypoblast did not develop the sickle-like orthotopic domain nor any other *Brachyury* expression domain in any of the ten investigated cases. The embryonic disc stayed bilaminar consisting of columnar, tall, epithelial-like epiblast cells and a thin underlying hypoblast layer (Fig. 4a, e). Sham-operated stage-1 embryos, in which the hypoblast layer was repositioned after having been lifted off, also stayed bilaminar but hypoblast cells took on a cuboidal shape (Fig. 4f). *Brachyury* expression in these sham operations varied between negative reactions (6/16; cf. Fig. 4b, f), weakly positive reactions distributed evenly across most of the embryonic disc (7/16), weakly positive reactions in a few single ectopic cells (2/16; Fig. 4b) and an orthotopic positive reaction (1/16).

At stage 2 a discernable effect of hypoblast ablation on *Brachyury* expression was detected in 13 of 16 cultured embryos. These cultures had an enlarged orthotopic *Brachyury* domain; the orthotopic domain was considered to be enlarged when the anterior tip extended further than half of the whole embryonic disc's diameter (Figs. 5b, c, 7). In six of these embryos *Brachyury* was additionally expressed in a branch- or arc-like ectopic pattern along the anterolateral circumference of the embryonic disc (Fig. 5b, c). In the orthotopic region both epiblast and mesoderm cells expressed *Brachyury* and the primitive streak region contained multiple layers of spindle-like mesoderm cells (Fig. 5h). In the branch-like antero-lateral domain the *Brachyury*-expressing cells were located in the mesoderm layer; the overlying epiblast expressed *Brachyury* less intensely or not at all (Fig. 5i). *Brachyury*-expressing mesoderm cells anterior to the tip of the orthotopic domain and an enlargement of the orthotopic *Brachyury* domain were not observed in any of the six controls. However, the control group developed well in culture and all embryos showed a rhombic expression pattern in the posterior elongated region of the disc (Fig. 5a) representing
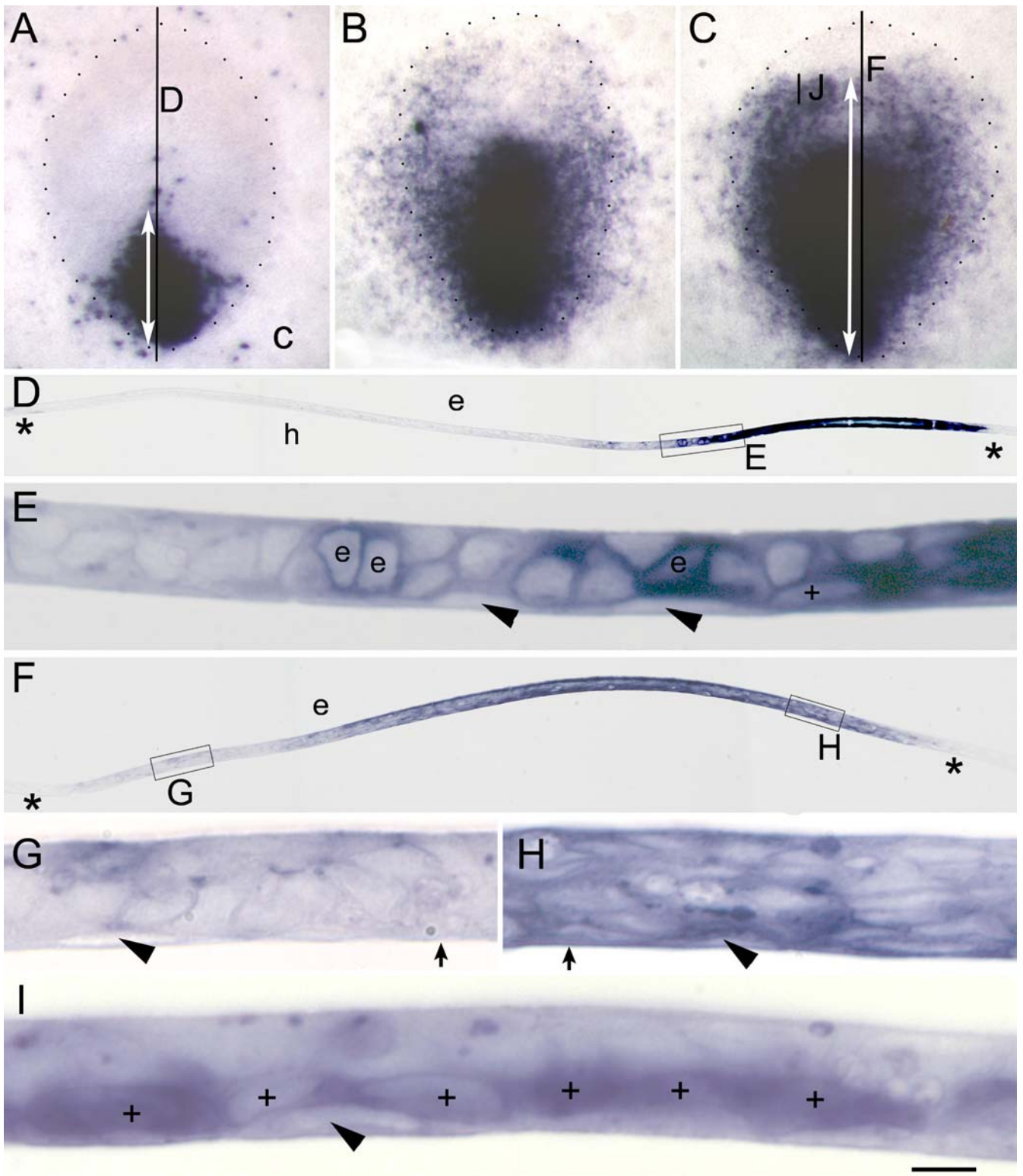
Fig. 5 *Brachyury* expression of cultured stage-2 rabbit embryos: en face views of embryos with hypoblast ablation (**b**, **c**) and of a control (**a**). *Bars* and *letters* indicate sections shown in **d**–**i**; other inscriptions and orientation of sections as in Fig. 3. Control embryos show an orthotopic *Brachyury* expression domain in the primitive streak (*white double arrow* in **a**) and regular stratification with cuboidal epiblast (*e*) and spindle-shaped mesoderm cells (+) expressing *Brachyury* while the hypoblast (*black arrowheads*) is free of expression. Crowded, multi-layered mesoderm cells are found in the enlarged streak in embryos with hypoblast removed (*white arrow* in **c**, **g**, **h**). Hypoblast cells can be found near the margins (*black arrowheads* in **g**, **h**) but not in central areas of the embryonic disc (*arrow* in **g**, **h**). Sections of the ectopic anterior domain (**i**) show mesoderm (+) but no epiblast cells (*e*) expressing *Brachyury*. *Scale bar* 150 μm in **a**–**c**; 60 μm in **d**, **f**; 10 μm in **e**, **g**, **h**; 7 μm in **i**
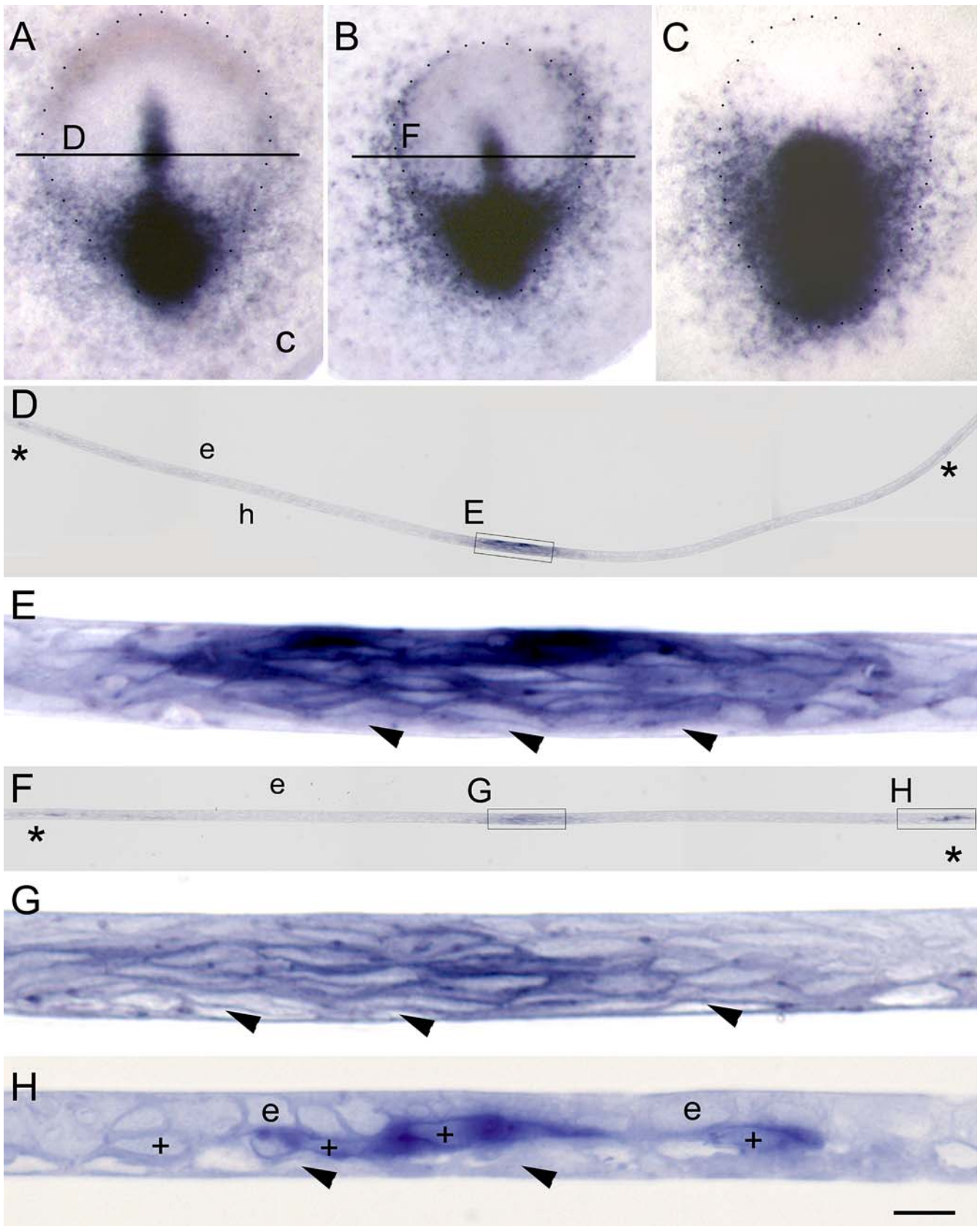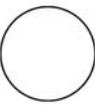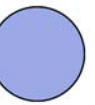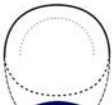
Fig. 6 *Brachyury* expression of cultured stage-3 rabbit embryos: en face views of embryos with hypoblast ablation (**b*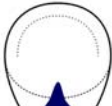*, **c**) and of a control (**a**). *Bars* and *letters* indicate sections shown in **d–h**; other inscriptions and orientation of sections as in Fig. 3. The morphology of the primitive node, characterized by multi-layered mesoderm cells, is similar in controls and after hypoblast removal (**e**, **g**). Mesoderm cells of the ectopic lateral domain at the border of the disc (**h**) strongly express *Brachyury* while epiblast (*e*) and hypoblast (*black arrowheads*) is free of expression in these compartments. *Scale bar* 240 μm in **a–c**; 80 μm in **d**, **f**; 12 μm in **e**, **g**, **h**

Fig. 7 Compilation of results obtained with cultured embryos after total hypoblast ablation, after ablation and re-implanting the hypoblast in the former position (sham operation; only stage 1) and with control embryos in the three experimental groups (stage 1, 2 and 3 at the start of culture). Orthotopic *Brachyury* expression domains are drawn in *dark blue*, coherent ectopic expression domains in *light blue*. To compare the expression patterns after culture with the in vivo condition, the dynamics of the physiological *Brachyury* expression pattern (Viebahn et al. 2002) is illustrated in the *left column* (*amc* anterior marginal crescent, *pge* posterior gastrula extension)

normally arranged epiblast and mesoderm cells in the primitive streak region (Fig. 5d, e).

At stage 3 an effect of hypoblast ablation on *Brachyury* expression in the embryonic disc was visible in 6 of 18 cultivated embryos: ectopic expression of *Brachyury* was observed in laterally located arc-like branches at the border of the embryonic disc and regarded as an expression located anteriorly to the orthotopic domain (Figs. 6b, c, f, h, 7). This domain was in general slim, consisted of 2–6 *Brachyury*-expressing mesoderm cells located next to one another and was smaller compared to the anterior ectopic domain observed in cultivated stage-2 embryos (Fig. 6h). The stratification in that region was regular with cuboidal epiblast cells dorsally and a discrete layer of hypoblast or endoderm cells ventrally. No expression was found in paraxial mesoderm cells between the node or prospective notochordal process, which had developed during the culture period, and the lateral *Brachyury*-expressing mesoderm cells. The orthotopic domain was laterally but not anteriorly enlarged in embryos with an ablated hypoblast when compared to the control embryos: three of seven controls developed to primitive node and early chorda stages and expressed *Brachyury* in the anterior part of the streak less intensely than in the remaining posterior part of the streak (Fig. 6a). In both controls and embryos with an ablated hypoblast, the node

area consisted of multi-layered mesoderm cells expressing *Brachyury* (Fig. 6c–f).

Discussion

In this report we extend the functional analysis of the hypoblast's role in mammalian mesoderm formation to the rabbit by applying microsurgical methods hitherto reserved for experimental analysis of the hypoblast in the chick embryo (cf. Bertocchini and Stern 2002). Hypoblast removal causes specific patterns of ectopic *Brachyury* expression and mesoderm formation in the epiblast in a stage-dependent fashion preceding primitive streak formation. As likely candidates for hypoblast signals controlling the mesoderm programme during the gastrulating process we confirmed the secreted Wnt and nodal antagonists Cer1 and Dkk1; the expression of these molecules delineates novel and complex hypoblast compartments which, taken together, fit the epiblast compartments apparently competent to engage in the mesoderm formation programme. From these results it follows that the hypoblast physiologically controls the expression of the mesoderm marker *Brachyury* and the generation of mesoderm cells in the mammalian epiblast. Consequently, before and during primitive streak formation, an additional programme must exist, possibly

executed within the epiblast, which controls the changing competence of specific epiblast compartments to form the mesoderm.

Evidence for hypoblast expression of Wnt and nodal antagonists to control mesoderm formation in the rabbit

The cloned rabbit cDNAs of *rbCer1* and *rbDkk1* show high homology to known mammalian sequences and their expression patterns support the view that they are the rabbit homologues. Although both expression patterns differ in detail, both genes are expressed in the future anterior half of the embryonic disc (already by 5.5 dpc, i.e. prior to morphological axial differentiation; cf. Idkowiak et al. 2004) and keep the shape of their characteristic expression compartments during pre- and early primitive streak development: the *rbCer1* domain fits well into the anterior and lateral outlines of the *rbDkk1*-free domain in the anterior centre of the embryo throughout this early period of expression. Interestingly, the anterior border of the clasp of *rbDkk1*-expressing hypoblast cells coincides with the anterior border of the prospective forebrain with the epidermal ectoderm, which is marked, for example, by expression of ANF in the overlying epiblast at stage 3 (Weisheit et al., in preparation). The *rbCer1* expression domain, on the other hand, coincides with the prospective forebrain territory inside the ANF domain. While it is intriguing to speculate on why the two signalling molecules are expressed by the same cell only in the small overlapping region of both compartments, their expression domains suggest a complementary role in mesoderm inhibition or neural plate induction and delineation; for example, the clasp-like *rbDkk1* domain may shield the central *rbCer1* domain from signals originating in the extraembryonic tissues.

Some aspects of the *rbCer1* and *Dkk1* expression domains described here have also been found in the mouse: for example, *Cer1* is expressed in a central domain of the visceral endoderm (VE; Belo et al. 1997), a region commonly defined as the distal visceral endoderm of the egg cylinder which shifts anteriorly during development (Thomas and Beddington 1996; Perea-Gomez et al. 2001a; Rivera-Perez et al. 2003). Similarly, posterolateral "branches" of the *Dkk1* expression domain are found in the mouse (Glinka et al. 1998; Perea-Gomez et al. 2001b). But a close association including the partial overlap of the two domains has not been demonstrated so far. Also, an expression domain in the primitive streak has not been described for either *Cer1* (Belo et al. 1997; Shawlot et al. 1998; Stanley et al. 2000) or for *Dkk1* (Glinka et al. 1998; Perea-Gomez et al. 2001b). The discrepancy of the results may well be functionally insignificant and possibly due to the small size and complex morphology (egg cylinder) or the fast development of the mouse embryo, respectively, at this stage. However, functionality could be inferred from the fact that *Cer1* and *Dkk1* expression in the hypoblast of the chick (Foley et al. 2000; Chapman et al. 2002) is comparable to the expression pattern in the rabbit and that *Cerl* plays a causal role in establishing axial polarity in the chick by positioning the primitive streak (Bertocchini and Stern 2002). Differences in hypoblast expression patterns between chick and rabbit are most likely due to the profoundly different developmental histories of the hypoblast between birds and mammals. While in many mammals hypoblast differentiates from the inner cell mass several days before gastrulation commences, in the chick various "generations" of hypoblast-like lower layer cells start to develop almost coincidently with mesoderm formation at the beginning of gastrulation (Bertocchini and Stern 2002; Callebaut et al. 2003). In fact, signs of a successive replacement of one sort of lower layer by another (e.g. primary hypoblast by endoblast), well described in the chick (Bertocchini and Stern 2002), have not been found so far in the mammalian embryo, although hypoblast cell movement to the anterior pole has been described in the mouse (Thomas and Beddington 1996; Yamamoto et al. 2004).

With the formation of the streak at stage 3 *Cer1* is strongly expressed in its rostral part and is later expressed in the entire primitive streak during streak elongation but downregulated at stage 4 (King and Brown 1999; Rodriguez-Esteban et al. 1999; Foley et al. 2000; Chapman et al. 2002). Similar to the *Cer1* patterns, *Dkk1* expression in the chick is associated with cells of the forming streak (resembling the appearance of the PGE in the rabbit) at HH stage 2 and is found at a higher concentration in the anterior part of the streak at stage 3 (Chapman et al. 2002). As both these inhibiting molecules are secreted proteins they likely play a role in patterning the epiblast epithelium, possibly by suppressing pathways involved in mesoderm generation. In *Xenopus*, for example, signalling molecules of the TGFβ superfamily, such as Vg1 and activin, are involved in mesoderm formation and axial differentiation (de Robertis et al. 2000) and, in the mouse, signalling through the TGFβ family member nodal acts as a master switch in mesoderm induction and primitive streak formation (Schier and Shen 2000). Gain-of-function experiments in the chick indicated that nodal signalling is able to induce ectopic primitive streaks after removal of the hypoblast (Bertocchini and Stern 2002) and in both mouse and chick nodal signalling is controlled by a Cer1 and Lefty1 antagonism necessary to coordinate the nodal-derived mesoderm cascade and leading to primitive streak formation in the posterior part of the embryo (Bertocchini and Stern 2002; Perea-Gomez et al. 2002; Yamamoto et al. 2004; see however Belo et al. 2000).

The function of *Dkk1* as a Wnt antagonist also points to another pathway of mesoderm induction, which suggests that Wnt signalling is necessary to induce and orchestrate mesoderm formation in vertebrates; misexpression of chicken Wnt8c in transgenic mice embryos causes axis duplication as a possible result of an additional ectopic primitive streak anlage (Pöpperl et al. 1997) and Vg1 is dependent on Wnt signalling in streak induction in the chick (Skromne and Stern 2001, 2002). Wnt3-deficient

mice do not form a primitive streak and lack mesoderm (Liu et al. 1999). Functionally, the mesoderm marker *Brachyury* is a direct target of β-catenin, which transmits Wnt signalling intracellulary (Huber et al. 1996; Arnold et al. 2000). Murine Dkk1 inhibits the axis-inducing xWnt8c in *Xenopus* embryos (Glinka et al. 1998) suggesting that it acts as a Wnt inhibitor like its *Xenopus* homologue which is able to antagonise the canonical Wnt pathway (transducing via intracellular β-catenin relocation) used by Wnt1, Wnt3a, Wnt2b and Wnt8 (Glinka et al. 1998; Krupnik et al. 1999; Kazanskaya et al. 2000; Wu et al. 2000).

The finding that both *rbCer1* and *rbDkk1* are also expressed in the streak might be interpreted as them exerting a regulatory effect on mesoderm generation and inhibiting an excessive production of mesoderm cells at the place of its generation. Notably, the putative antagonising effect of *rbCer1* and *rbDkk1* is situated in the epiblast cells that are getting transformed and in the mesoderm cells that were transformed, suggesting a need for an auto-inhibitory influence. As in the anterior half of the hypoblast, both expression compartments are complementary to each other. Here in the streak, their differential expression mirrors anterior-posterior differences in the developmental history of the streak exemplified not least by the differential early *Brachyury* expression that can be observed in chick and rabbit (cf. Viebahn et al. 2002).

The rabbit hypoblast suppresses mesoderm generation in a stage-dependent fashion

Our loss-of-function experiments present strong evidence that the rabbit hypoblast regulates mesoderm formation in the epiblast. If left undisturbed prior to culture the hypoblast seems to be most efficient in preventing *Brachyury* expression being switched on in the epiblast (Fig. 4a) while lifting off and repositioning the hypoblast (sham operations) is slightly less efficient: in some cases, *Brachyury* is "allowed" to be switched on just up to a mosaic-like pattern (Fig. 4b) in a manner similar to the one known from the physiological start of *Brachyury* expression (Viebahn et al. 2002). Importantly, the disc-shaped morphology and the possibility to distinguish, immediately prior to streak formation, two stages with a discernible axial polarity helped to reveal that compartments exist in the epiblast with different capacities to form mesoderm and that the epiblast's competence to form mesoderm has a narrow time window.

At stage 1, with the beginning of morphological axial differentiation, all epiblast cells are principally able to transform into mesoderm cells as the most striking effects after hypoblast removal show an ectopic *Brachyury* expression domain all over the disc and multi-layered mesoderm cells in the whole area of *Brachyury* expression. Not all (only 4 of 27) cultured embryos developed this maximal response to hypoblast removal and differences in the extent of *Brachyury* expression might have methodological reasons: (1) small islands of hypoblast

tissue may unintentionally have not been completely removed; (2) the hypoblast may have grown again from the cut edge near the yolk-sac epithelium; and (3) younger stages of development react to the culture conditions in different ways as compared to older stages. The first possibility is unlikely as the hypoblast is invested with a prominent intermediate filament cytoskeleton and substantial desmosome-like intercellular contacts (Viebahn et al. 1995) which makes it a coherent piece of tissue, especially when manipulated; moreover, the completeness of the removal is easily controlled visually during and after the operation due to the different appearance of the embryonic disc with and without hypoblast (Fig. 1). The second possibility seems to be supported by the presence of lower layer cells in several manipulated embryonic discs (Figs. 4i, j, 5g–i, 6e, g, h) but these cells apparently did not prevent the effects caused by the lack of hypoblast at the time following the operation; if at all, they may have hindered actual mesoderm formation, which follows *Brachyury* expression, as frequently seen, e.g in the ectopic domain anterior to the primitive streak (cf. Fig. 4i). Regarding the third possibility, it is to be noted that the culturing technique was originally introduced to culture (manipulated) chick embryos (New 1955) which are generally larger, more robust, and easier to handle than mammalian embryos. Nevertheless, this study showed that rabbit embryos can be successfully cultured in pre-streak and early streak stages; from late streak stages they also develop to early notochord and somite stages (this study and Fischer et al. 2002). Therefore, more likely reasons for the different responses of the epiblast are (1) a general difference in competence (being higher in the centre than at the periphery of the epiblast), and (2) a possible narrow time-window of epiblast responsiveness: the cultured embryos were very likely not at exactly the same substage at the time of hypoblast removal. The development from stage 1 to stage 2 (and to stage 3) is a gentle transition taking about 6 h. Responsiveness of the epiblast may last for only 1–2 h and epiblast cells of late stage-1 embryos are no longer responsive to mesoderm-inducing signals. Both competence characteristics could easily be controlled by extraembryonic factors, i.e. by a gradient of signalling originating in the trophoblast epithelium (attached to the embryonic disc peripherally in the epiblast layer) or in the yolk-sac epithelium (the lower layer of the extraembryonic tissue at the level of the hypoblast).

The development of *Brachyury* expression in the controls of stage-1 embryos points to another functional facet of the initiation of the mesoderm-forming programme. None of the unmanipulated stage-1 embryos and only one of the sham-operated ones express *Brachyury* in the orthotopic domain, i.e. they are not able to form the characteristic *Brachury* expression in the PGE in vitro with the hypoblast still present. This may be a sign of impaired cellular migration in the epiblast on the agarose substrate which would fit the postulated requirement of epiblast migration away from the anterior and central zones of high proliferation (Viebahn et al. 2002). In agreement with the concept for turning on the mesoderm

formation programme through a drop in proliferation as shown for *Drosophila* (cf. Seher and Leptin 2000) an essential step for initiating the mesoderm forming process in mammals was thought to be a reduction of the proliferation rate in the PGE (Viebahn et al. 2002). Removal or impairment of the hypoblast would then fulfill this requirement and turn on *Brachyury* expression (as the "master switch" for mesoderm formation); the spatial distribution of the epiblast's competence to do so might reflect local proliferation rates in the epiblast at the start of the culture.

In cultivated stage-2 embryos with an ablated hypoblast most of the embryos developed an enlarged orthotopic domain combined with an enlarged primitive streak. Additional *Brachyury* expression was found in mesoderm cells arranged in branch-like wings reaching from the orthotopic domain into the anterolateral part of the embryo. Notably, the overlying epiblast very rarely, if at all, expressed *Brachyury*. This indicates, firstly, that at stage 2 epiblast outside the prospective streak area (the PGE) is not capable of switching on *Brachyury* and, secondly, that the anterolateral mesoderm cells did not switch off *Brachyury* expression as they normally do during their movement from the streak to the lateral and anterior regions of the embryo. These findings suggest that the hypoblast has regulatory influence on epithelio-mesenchymal transition at a point in development where the course of streak formation is set but a fine-tuning of the extent of mesoderm generation, and possibly meso-derm movement, still has to be carried out. In cultivated stage-3 embryos the influence of hypoblast removal on mesoderm generation decreases, as the primitive streak was not as excessively enlarged when compared to the control embryos and when compared to enlargement of the orthotopic region observed in stage-2 embryos; the competence of the epiblast seems to be even further reduced than at stage 2. Possibly, epiblast at stage 3 is already completely committed to form neuroectoderm or epidermal ectoderm.

The effect of the hypoblast on mesoderm generation has been examined in other model organisms of vertebrate development, namely mouse and chick. Our findings agree with these results to a certain extent but several differences are also evident. Classical experiments in chick showed that 90° hypoblast rotation can induce an additional primitive streak arising from the grafted position (Wad-dington 1933). New insights into these patterning mechanisms revealed that the chick hypoblast does not change cell fates but influences cell movements in the epiblast (Foley et al. 2000). Complete hypoblast removal in pre-gastrula stages (stage 7 and 8) induced additional primitive streaks and, consequently, multiple axes to form; antagonising nodal activity, mediated by *Cerberus* being expressed in the hypoblast, could rescue the formation of additional streaks in the chick (Bertocchini and Stern 2002). In these experiments, an enlargement of the primitive streaks (both orthotopic and ectopically induced) and an excess of mesoderm formation has not been observed, nor was there any other ectopic formation of

mesoderm or expression of mesoderm markers outside the primitive streak regions (Bertocchini and Stern 2002). Principal differences in the developmental history of the hypoblast between mammals and birds referred to above might account for this effect.

Due to the complex architecture of the mouse egg-cylinder, manipulations are more difficult than in the rabbit and, moreover, a convenient analysis of the resulting spatial patterning is hindered. Therefore, explant recombination assays had been carried out to test the inductive (or suppressive) potential of the mouse VE (Kimura et al. 2000; Perea-Gomez et al. 2001b). These studies revealed that the AVE of gastrulating mouse embryos if grafted on explants of embryonic ectoderm suppressed the expression of the mesoderm markers *Brachyury* and *Cripto* (Kimura et al. 2000). The com-pound mutant mouse lacking the nodal antagonists mCer1 and Lefty1, both expressed in the VE, develops a primitive streak ectopically, indicating that also in mammals nodal is required for streak development and is antagonised by Cer1 and Lefty1 signalling; moreover, abnormal streaks were observed in the double knock-outs suggesting that they possess important roles in correct patterning of primitive streak and mesoderm formation (Perea-Gomez et al. 2002). Functionally, nodal induces cell migration of distal VE cells while the antagonists Cerl and Lefty1 suppress nodal signalling at the future anterior pole of the embryo and so regulate the formation of the anterior-posterior axis (Yamamoto et al. 2004). It will be important to describe the equivalent hypoblast movements in the rabbit, not least to find out whether they could be equivalent also to the dynamics of lower layer movements and replacement in the chick (Bertocchini and Stern 2002).

Although the molecular nature of the initiation of streak formation has been uncovered in chick and mouse, localisation of molecular events before and at the onset of gastrulation are just beginning to be described in the mammalian embryo (cf. Rivera-Perez et al. 2003; Perea-Gomez et al. 2004; Tam and Gad 2004). Our results provide evidence that the master switch of the mesoderm programme leading to streak development posteriorly, and hence axis formation, is turned on with the development of the PGE at stage 2. At earlier stages, when the anterior pole of the disc is visible due to the AMC (stage 1), all epiblast cells are principally able to transform into mesoderm cells; at this stage the axis of the embryo is defined (in the AMC) but still needs to be irrevocably fixed in the epiblast through the influence of the hypo-blast. Beyond stage 2 the hypoblast's influence on mesoderm formation decreases, but it still has a regulatory impact on mesoderm generation and patterning. These axial patterns and the time-dependent outcome of our experiments thus support the usefulness of distinguishing two closely connected stages preceding primitive streak formation in mammals.

604

References

Ang SL, Wierda A, Wong D, Stevens KA, Cascio S, Rossant J, Zaret KS (1993). The formation and maintenance of the definitive endoderm lineage in the mouse—involvement of HNF3/forkhead proteins. Development 119:1301–1315

Arnold SJ, Stappert J, Bauer A, Kispert A, Herrmann BG Kemler R (2000) *Brachyury* is a target gene of the Wnt/beta-catenin signaling pathway. Mech Dev 91:249–258

Barnes JD, Crosby JL, Jones CM, Wright CVE, Hogan BLM (1994) Embryonic expression of lim-1, the mouse homolog of *Xenopus* XLim-1, suggests a role in lateral mesoderm differentiation and neurogenesis. Dev Biol 161:168–178

Beddington RS, Robertson EJ (1998) Anterior patterning in mouse. Trends Genet 14:277–284

Beddington RS, Robertson EJ (1999) Axis development and early asymmetry in mammals. Cell 96:195–209

Bellairs R (1986) The primitive streak. Anat Embryol 174:1–14

Belo JA, Bouwmeester T, Leyns L, Kertesz N, Gallo M, Follettie M, De Robertis EM (1997) Cerberus-like is a secreted factor with neutralizing activity expressed in the anterior primitive endoderm of the mouse gastrula. Mech Dev 68:45–57

Belo JA, Bachiller D, Agius E, Kemp C, Borges AC, Marques S, Piccolo S, De Robertis EM (2000) Cerberus-like is a secreted BMP and nodal antagonist not essential for mouse development. Genesis 26:265–270

Bertocchini F, Stern CD (2002) The hypoblast of the chick embryo positions the primitive streak by antagonizing nodal signaling. Dev Cell 3:735–744

Biben C, Stanley E, Fabri L, Kotecha S, Rhinn M, Drinkwater C, Lah M, Wang CC, Nash A, Hilton D, Ang SL, Mohun T, Harvey RP (1998) Murine cerberus homologue mCer-1: a candidate anterior patterning molecule. Dev Biol 194:135–151

Blum M, Gaunt SJ, Cho KWY, Blumberg B, Steinbeisser H, Bittner D, De Robertis EM (1992) Gastrulation in the mouse: the role of the homeobox gene *goosecoid*. Cell 69:1097–1106

Bouwmeester T, Kim SH, Sasai Y, Lu B, De Robertis EM (1996) Cerberus is a head-inducing secreted factor expressed in the anterior endoderm of Spemann's organizer. Nature 382:595–601

Callebaut M., Van Nueten E, Bortier H, Harrisson F (2003) Positional information by Rauber's sickle and a new look at the mechanisms of primitive streak initiation in avian blastoderms. J Morphol 255:315–327

Chapman SC, Schubert FR, Schoenwolf GC, Lumsden A (2002). Analysis of spatial and temporal gene expression patterns in blastula and gastrula stage chick embryos. Dev Biol 245:187–199

Conlon FL, Lyons KM, Takaesu N, Barth KS, Kispert A, Herrmann B, Robertson EJ (1994) A primary requirement for nodal in the formation and maintenance of the primitive streak in the mouse. Development 120:1919–1928

Filosa S, Rivera-Perez JA, Gomez AP, Gansmuller A, Sasaki H, Behringer RR, Ang SL (1997) Goosecoid and HNF-3beta genetically interact to regulate neural tube patterning during mouse embryogenesis. Development 124:2843–2854

Fischer A, Viebahn C, Blum M (2002) FGF8 acts as a right determinant during establishment of the left-right axis in the rabbit. Curr Biol 12:1807–1816

Foley AC, Skromne I, Stern CD (2000) Reconciling different models of forebrain induction and patterning: a dual role for the hypoblast. Development 127:3839–3854

Glinka A, Wu W, Delius H, Monaghan AP, Blumenstock C, Niehrs C (1998) Dickkopf-1 is a member of a new family of secreted proteins and functions in head induction. Nature 391:357–362

Hay ED (1995) An overview of epithelio-mesenchymal transformation. Acta Anat 154:8–20

Huber O, Bierkamp C, Kemler R (1996) Cadherins and catenins in development. Curr Opin Cell Biol 8:685–691

Idkowiak J, Weisheit G, Viebahn C (2004) Polarity in the rabbit embryo. Semin Cell Dev Biol 15:607–617

Kazanskaya O, Glinka A, Niehrs C (2000) The role of *Xenopus dickkopf1* in prechordal plate specification and neural patterning. Development 127:4981–4992

Kimura C, Yoshinaga K, Tian E, Suzuki M, Aizawa S, Matsuo I (2000) Visceral endoderm mediates forebrain development by suppressing posteriorizing signals. Dev Biol 225:304–321

King T, Brown NA (1999) Developmental biology. Antagonists on the left flank. Nature 401:222–223

Knoetgen H, Teichmann U, Wittler L, Viebahn C, Kessel M (2000) Anterior neural induction by nodes from rabbits and mice. Dev Biol 225:370–380

Krupnik VE, Sharp JD, Jiang C, Robison K, Chickering TW, Amaravadi L, Brown DE, Guyot D, Mays G, Leiby K, Chang B, Duong T, Goodearl AD, Gearing DP, Sokol SY, McCarthy SA (1999) Functional and structural diversity of the human *Dickkopf* gene family. Nature 401:243–251

Liu P, Wakamiya M, Shea MJ, Albrecht U, Behringer RR, Bradley A (1999) Requirement for Wnt3 in vertebrate axis formation. Nat Genet 22:361–365

Lowe LA, Supp DM, Sampath K, Yokoyama T, Wright CVE, Potter SS, Overbeek P, Kuehn MR (1996) Conserved left-right asymmetry of nodal expression and alterations in murine situs inversus. Nature 381:158–161

Meno C, Saijoh Y, Fujii H, Ikeda M, Yokoyama T, Yokoyama M, Toyoda Y, Hamada H (1996) Left-right asymmetric expression of the TGF beta-family member lefty in mouse embryos. Nature 381:151–155

Monaghan AP, Kaestner KH, Grau E, Schütz G (1993) Post-implantation expression patterns indicate a role for the mouse forkhead/hnf-3 alpha, beta and gamma genes in determination of the definitive endoderm, chordamesoderm and neuroectoderm. Development 119:567–578

New DAT (1955) A new technique for the cultivation of the chick embryo in vitro. J Embryol Exp Morphol 3:326–331

Oulad-Abdelghani M, Chazaud C, Bouillet P, Mattei MG, Dolle P, Chambon P (1998) Stra3/lefty, a retinoic acid-inducible novel member of the transforming growth factor-beta superfamily. Int J Dev Biol 42:23–32

Pearce JJ, Penny G, Rossant J (1999) A mouse cerberus/Dan-related gene family. Dev Biol 209:98–110

Perea-Gomez A, Lawson KA, Rhinn M, Zakin L, Brulet P, Mazan S, Ang SL (2001a) Otx2 is required for visceral endoderm movement and for the restriction of posterior signals in the epiblast of the mouse embryo. Development 128:753–765

Perea-Gomez A, Rhinn M, Ang SL (2001b) Role of the anterior visceral endoderm in restricting posterior signals in the mouse embryo. Int J Dev Biol 45:311–320

Perea-Gomez A, Vella FD, Shawlot W, Oulad-Abdelghani M, Chazaud C, Meno C, Pfister V, Chen L, Robertson E, Hamada H, Behringer RR, Ang SL (2002) Nodal antagonists in the anterior visceral endoderm prevent the formation of multiple primitive streaks. Dev Cell 3:745–756

Perea-Gomez A, Camus A, Moreau A, Grieve K, Moneron G, Dubois A, Cibert C, Collignon J (2004) Initiation of gastrulation in the mouse embryo is preceded by an apparent shift in the orientation of the anterior-posterior axis. Curr Biol 14:197–207

Pöpperl H, Schmidt C, Wilson V, Hume CR, Dodd J, Krumlauf R, Beddington RSP (1997) Misexpression of Cwnt8C in the mouse induces an ectopic embryonic axis and causes a truncation of the anterior neuroectoderm. Development 124:2997–3005

Rivera-Perez JA, Mager J, Magnuson T (2003) Dynamic morphogenetic events characterize the mouse visceral endoderm. Dev Biol 261:470–487

de Robertis EM, Larrain J, Oelgeschlager M, Wessely O (2000) The establishment of Spemann's organizer and patterning of the vertebrate embryo. Nat Rev Genet 1:171–181

Rodriguez-Esteban C, Capdevila J, Economides AN, Pascual J, Ortiz A, Izpisua Belmonte JC (1999) The novel Cer-like protein Caronte mediates the establishment of embryonic left-right asymmetry. Nature 401:243–251

Sasaki H, Hogan BLM (1993) Differential expression of multiple fork head related genes during gastrulation and axial pattern formation in the mouse embryo. Development 118:47–59

Schier AF, Shen MM (2000) Nodal signalling in vertebrate development. Nature 403:385–389

Seher TC, Leptin M (2000) Tribbles, a cell-cycle brake that coordinates proliferation and morphogenesis during *Drosophila* gastrulation. Curr Biol 10:623–629

Shawlot W, Behringer RR (1995) Requirement for lim1 in head-organizer function. Nature 374:425–430

Shawlot W, Deng JM, Behringer RR (1998) Expression of the mouse cerberus-related gene, *Cerr1*, suggests a role in anterior neural induction and somitogenesis. Proc Natl Acad Sci USA 95:6198–6203

Skromne I, Stern CD (2001) Interactions between Wnt and Vg1 signalling pathways initiate primitive streak formation in the chick embryo. Development 128(15):2915–2927

Skromne I, Stern CD (2002) A hierarchy of gene expression accompanying induction of the primitive streak by Vg1 in the chick embryo. Mech Dev 114:115–118

Stanley EG, Biben C, Allison J, Hartley L, Wicks IP, Campbell IK, McKinley M, Barnett L, Koentgen F, Robb L, Harvey RP (2000) Targeted insertion of a lacZ reporter gene into the mouse Cer1 locus reveals complex and dynamic expression during embryogenesis. Genesis 26:259–264

Tam PPL, Gad JM (2004) Gastrulation in the mouse. In: Stern CD (ed) Gastrulation. Cold Spring Harbor Laboratory Press, Cold Spring Harbor (in press)

Thomas PQ, Beddington RSP (1996) Anterior primitive endoderm may be responsible for patterning the anterior neural plate in the mouse embryo. Curr Biol 6:1487–1496

Thomas PQ, Brown A, Beddington RSP (1998). *Hex*: a homeobox gene revealing peri-implantation asymmetry in the mouse embryo and an early transient marker of endothelial cell precursors. Development 125:85–94

Varlet I, Collignon J, Robertson EJ (1997) *nodal* expression in the primitive endoderm is required for specification of the anterior axis during mouse gastrulation. Development 124:1033–1044

Viebahn C (1995) Epithelio-mesenchymal transformation during formation of the mesoderm in the mammalian embryo. Acta Anat 154:79–97

Viebahn C, Mayer B, Miething A (1995) Morphology of incipient mesoderm formation in the rabbit embryo: a light- and retrospective electron-microscopic study. Acta Anat 154:99–110

Viebahn C, Stortz C, Mitchell SM, Blum M (2002) Low proliferative and high migratory activity in the area of *Brachyury* expressing mesoderm progenitor cells in the gastrulating rabbit embryo. Development 129:2355–2365

Waddington CH (1933) Induction by the primitive streak and its derivatives in the chick. J Exp Biol 10:38–46

Weinstein DC, Hemmati-Brivanlou A (1999) Neural induction. Annu Rev Cell Dev Biol 15:411–433

Weisheit G, Mertz KD, Schilling K, Viebahn C (2002) An efficient in situ hybridization protocol for multiple tissues sections and probes on miniaturized slides. Dev Genes Evol 212:403–406

Wodarz A, Hinz U, Engelbert M, Knust E (1995) Expression of crumbs confers apical character on plasma membrane domains of ectodermal epithelia of *Drosophila*. Cell 82:67–76

Wu W, Glinka A, Delius H, Niehrs C (2000) Mutual antagonism between dickkopf1 and dickkopf2 regulates Wnt/beta-catenin signalling. Curr Biol 10:1611–1614

Yamamoto M, Saijoh Y, Perea-Gomez A, Shawlot W, Behringer RR, Ang SL, Hamada H, Meno C (2004) Nodal antagonists regulate formation of the anteroposterior axis of the mouse embryo. Nature 428:387–392

Yokouchi Y, Vogan KJ, Pearse RV, Tabin CJ (1999) Antagonistic signaling by *Caronte*, a novel Cerberus-related gene, establishes left-right asymmetric gene expression. Cell 98:573–583